"$\gamma + jet$" EVENT RATE ESTIMATION FOR GLUON DISTRIBUTION DETERMINATION AT THE TEVATRON RUN II.

D.V. Bandurin, N.B. Skachkov

Laboratory of Nuclear Problems, JINR, Dubna, Russia

Abstract

Since a lot of theoretical predictions on the production of new particles (Higgs, SUSY) at the Tevatron are based on model estimations of the proton gluon density behavior at low x and high values of a transfered momentum Q^2, the study of a possibility of a measurement of the gluon density in this kinematic region directly in Tevatron experiments is obviously of a big interest [1].

Basing on the selection criteria proposed ealier in [1] and [2], the background events suppression factors and corresponding signal events selection efficiencies are determined here. The estimation of the number of "$\gamma + jet$" events suitable for measurement of gluon distribution in different x and Q^2 intervals at Tevatron Run II is also done.

It is shown that with integrated luminosity $L_{int} = 3\ fb^{-1}$ it would be possible to collect about one million of these events. This number would allow to cover a new kinematical region, $10^{-3} < x < 1.0$ with $1.6 \cdot 10^3 \leq Q^2 \leq 2 \cdot 10^4\ (GeV/c)^2$, not studied in any previous experiment. This area includes the values of Q^2 that are, on the average, by about one order of magnitude higher than those reached at HERA now. The rates of $g\,c \rightarrow \gamma^{dir} + jet$ events are also obtained.

Key-words: gluon distribution, proton, direct photon

1   Selection cuts and background suppression.

To estimate the efficiency of the selection criteria used in [1]–[5] we carried out the simulation [1] with a mixture of all QCD and SM subprocesses with large cross sections existing in PYTHIA [6] (namely, in notations of PYTHIA, with ISUB=1, 2, 11–20, 28–31, 53, 68). The events caused by this set of the subprocesses may give a large background to the "$\gamma^{dir} + jet$" signal events defined by the subprocesses (1) and (2) [2]:
"Compton-like" scattering

$$qg \rightarrow q + \gamma \tag{1}$$

and "annihilation" process

$$q\overline{q} \rightarrow g + \gamma \tag{2}$$

(ISUB=29 and 14) that were also included in the performed simulation.

Three generations with the above-mentioned set of subprocesses were done. Each of them was fulfilled with a different value of the PYTHIA parameter $CKIN(3) \equiv \hat{p}_{\perp}^{min}$ that defines the minimal value of parton P_t appearing in the final state of a hard $2 \rightarrow 2$ parton level fundamental subprocess in the case of the initial state radiation (ISR) absence. These values were $\hat{p}_{\perp}^{min} = 40, 70$ and $100\ GeV/c$. By 40 million events were generated for each of

---

[1] PYTHIA 5.7 version with default CTEQ2L parameterization of structure functions is used here.

[2] A contribution of another possible NLO channel $gg \rightarrow g\gamma$ (ISUB=115 in PYTHIA) was found to be still negligible even at Tevatron energies.

the $\hat{p}_\perp^{min}$ value. The cross sections of the above-mentioned subprocesses define the rates of the corresponding physical events and, thus, serve during a simulation as weight factors.

We selected "γ^{dir}-candidate $+1$ jet" events containing one γ^{dir}-candidate (denoted in what follows as $\tilde{\gamma}$) and one jet (found by a subroutine LUCELL implemented in PYTHIA as a jetfinder) with $P_t^{jet} > 30\, GeV/c$. Here and below, as we work at the PYTHIA particle level of simulation, speaking about the γ^{dir}-candidate we actually mean, apart from γ^{dir}, a set of particles like electrons, bremsstrahlung photons and also photons from neutral meson decays that may be registered in one D0 calorimeter [3] cell of the $\Delta\eta \times \Delta\phi = 0.1 \times 0.1$ size.

Below we consider a set of 17 cuts that are separated into 2 subsets: a set of the "photonic" cuts and a set of the "hadronic" ones. The first set consists of 5 cuts used to select an isolated photon candidate in some $P_t^{\tilde{\gamma}}$ interval. The second one, that includes 12 cuts, deals mostly with jets and clusters and is used to select events having one "isolated jet" and a limited P_t activity out of "$\tilde{\gamma} + jet$" system.

All of the cuts are listed in Table 1. Their influence on the signal-to-background ratio S/B is presented in Table 2 (for a case of the most illustrative intermediate interval of event generation with $\hat{p}_\perp^{min} = 70\, GeV/c$) and Tables 3–5.

Tables 1 and 2 are complementary to each other. The numbers in the left-hand column ("Cut") of Table 2 coincide with the numbers of cuts listed in Table 1.

The second and third columns of Table 2 contain, respectively, the numbers of signal direct photons (S) and background $\gamma^{dir}-$candidates (B) left in the sample of events after application of each cut from Table 1. The numbers of background events B do not include events with electrons that fake photon signal. Their numbers in the samples are presented separately in the last right-hand column "$e^{\pm}$". The other columns of Table 2 include the values of efficiencies $Eff_{S(B)}$ (with their errors) defined as a ratio of a number of the signal (background) events that passed under each of the cuts (1–17) to the number of the preselected events (1st cut of this table). They are followed by the column containing the values of S/B ratio.

Table 1: List of the applied cuts (will be used also in Tables 2–5).

1. a) $P_t^{\tilde{\gamma}} \geq 40\, GeV/c$, b) $P_t^{jet} \geq 30\, GeV/c$,	**9.** $\Delta\phi < 17°$;
c) $|\eta^{\tilde{\gamma}}| \leq 2.5$, d) $P_t^{hadr} < 7\, GeV/c\,^*$;	**10.** $P_t^{miss}/P_t^{\tilde{\gamma}} \leq 0.10$;
2. $P_t^{isol} \leq 5\, GeV/c$, $\epsilon^{\tilde{\gamma}} < 15\%$;	**11.** $P_t^{clust} < 20\, GeV/c$;
3. $P_t^{\tilde{\gamma}} \geq \hat{p}_\perp^{min}$;	**12.** $P_t^{clust} < 15\, GeV/c$;
4. $P_{t_{ring}}^{isol} \leq 1\, GeV/c\,^{**}$;	**13.** $P_t^{clust} < 10\, GeV/c$;
5. $P_t^{isol} \leq 2\, GeV/c$, $\epsilon^{\tilde{\gamma}} < 5\%$;	**14.** $P_t^{out} < 20\, GeV/c$;
6. $Njet \leq 3$;	**15.** $P_t^{out} < 15\, GeV/c$;
7. $Njet \leq 2$;	**16.** $P_t^{out} < 10\, GeV/c$;
8. $Njet = 1$;	**17.** $e^{jet} \leq 3\%$.

$*$ maximal P_t of a hadron in the ECAL cell containing a γ^{dir}-candidate;

$**$ A scalar sum of P_t in the ring: $P_t^{sum}(R = 0.4) - P_t^{sum}(R = 0.2)$.

Line number 1 of Table 1 contains four primary preselection criteria. It includes general P_t cuts (1a), (1b) as well as the cut connected with the D0 electromagnetic calorimeter (ECAL) geometry (1c) and the cut (1d) that excludes γ^{dir}-candidates accompanied by hadrons entering the same calorimeter cell as $\tilde{\gamma}$.

Line number 2 of Table 1 fixes the values of γ^{dir}-candidate isolation parameters P_t^{isol} and $\epsilon^{\tilde{\gamma}}$, i.e. the value of the scalar sum of P_t of all particles surrounding γ^{dir}-candidate

---

[3]The geometry of D0 detector was used in the simulation [7].

within a cone of $R^{\gamma}_{isol} = ((\Delta\eta)^2 + (\Delta\phi)^2)^{1/2} = 0.7$ and its fraction $\epsilon^{\tilde{\gamma}} = P_t^{isol}/P_t^{\tilde{\gamma}}$.

The third cut selects the events with γ^{dir}-candidate having P_t higher than $\hat{p}_\perp^{min}$ threshold. We impose this cut to select the samples of events with $P_t^{\tilde{\gamma}} \geq 40, 70$ and $100\ GeV/c$ as ISR may smear the sharp kinematical cutoff defined by $CKIN(3)$ [6]. This cut reflects an experimental viewpoint when one is interested in how many events with γ^{dir}-candidates are contained in some definite interval of $P_t^{\tilde{\gamma}}$.

The forth cut restricts a value of $P_{t_{ring}}^{isol} = P_{tR=0.4}^{isol} - P_{tR=0.2}^{isol}$, where P_{tR}^{isol} is a sum of P_t of all ECAL cells contained in the cone of the radius R around the cell fired by γ^{dir}-candidate [8], [9].

The fifth cut makes tighter the isolation criteria within $R = 0.7$ than those imposed onto γ^{dir}-candidate in the second line of Table 1.

Table 2: Values of significance and efficiencies for $\hat{p}_\perp^{min} = 70\ GeV/c$.

Cut	S	B	$Eff_S(\%)$	$Eff_B(\%)$	S/B	$e^\pm$
1	39340	1247005	100.00± 0.00	100.000± 0.000	0.03	17562
2	36611	51473	93.06± 0.68	4.128± 0.019	0.71	4402
3	29903	18170	76.01± 0.58	1.457± 0.011	1.65	2038
4	26426	11458	67.17± 0.53	0.919± 0.009	2.31	1736
5	23830	7504	60.57± 0.50	0.602± 0.007	3.18	1568
6	23788	7406	60.47± 0.50	0.594± 0.007	3.21	1554
7	23334	6780	59.31± 0.49	0.544± 0.007	3.44	1460
8	19386	4136	49.28± 0.43	0.332± 0.005	4.69	1142
9	18290	3506	46.49± 0.42	0.281± 0.005	5.22	796
10	18022	3418	45.81± 0.41	0.274± 0.005	5.27	210
11	15812	2600	40.19± 0.38	0.208± 0.004	6.08	176
12	13702	1998	34.83± 0.35	0.160± 0.004	6.86	130
13	10724	1328	27.26± 0.30	0.106± 0.003	8.08	88
14	10636	1302	27.04± 0.30	0.104± 0.003	8.17	86
15	10240	1230	26.03± 0.29	0.099± 0.003	8.33	84
16	8608	984	21.88± 0.26	0.079± 0.003	8.75	64
17	6266	622	15.93± 0.22	0.050± 0.002	10.07	52

($*$) The background (B) does not include the contribution from the "$e^\pm$ events" (i.e. in which $e^\pm$ fake γ-candidate) that is shown separately in the right-hand column "$e^\pm$".

The cuts considered up to now, apart from general preselection cut $P_t^{jet} \geq 30\ GeV/c$, used in the first line of Table 1, were connected with photon selection ("photonic" cuts).

The cuts 6–9 are connected with the selection of events having only one jet and the definition of jet-photon spatial orientation in ϕ-plane. The 9-th cut selects the events with jet and photon transverse momenta being "back-to-back" to each other in ϕ−plane within the angle interval of the $\Delta\phi = 17°$ size [4].

In line 10 we used the cut on P_t^{miss} to reduce the background contribution from the electroweak subprocesses $q\,g \to q' + W^\pm$ and $q\,\bar{q}' \to g + W^\pm$ with the subsequent decay $W^\pm \to e^\pm\nu$ that leads to a substantial P_t^{miss} value (see plots in [4]). One can see from the last column of Table 2 "$e^\pm$" that the cut on P_t^{miss} reduces strongly (in about 4 times) the number of events containing $e^\pm$ as direct photon candidate.

Moving further we see from Table 2 that the cuts 11–16 of Table 1 reduce the values of transverse momenta of clusters (mini-jets) P_t^{clust} and the modulus of a vector sum of

---
[4]i.e. within the size of three calorimeter cells

all particles that are not included into the "$\tilde{\gamma} + jet$" system, i.e. P_t^{out}, down to the values less than 10 GeV/c. The 17-th cut of Table 1 imposes the jet isolation requirement. It leaves only the events with jets having the sum of P_t in the ring of the $\Delta R = 0.3$ size surrounding a jet to be less than 3% of P_t^{jet}. From comparison of the numbers in the 10-th and 17-th lines we make an important conclusion that all these new cuts (11–17) may lead to the following about two-fold improvement of S/B ratio [5]. This improvement is achieved due to a reduction of P_t activity out of "$\tilde{\gamma} + jet$" system [6].

It is also important to mention that *the total effect of "hadronic cuts" 6–17 for the case of $\hat{p}_\perp^{min} = 70$ GeV/c consists of about twelve-fold decrease of background contribution at the cost of less than four-fold loss of signal events (what results in about 3.2 times growth of S/B ratio).* So, in this sense, we may conclude that from the viewpoint of S/B ratio a study of "$\gamma + jet$" events may be more preferable as compared with a case of inclusive photon production.

Table 3: Number of signal and background events remained after cuts.

$\hat{p}_\perp^{min}$		γ	γ	photons from the mesons				
(GeV/c)	Cuts	direct	brem	π^0	η	ω	K_S^0	$e^\pm$
	Preselected	18056	14466	152927	56379	17292	14318	2890
40	After cuts	6238	686	824	396	112	104	24
	+ jet isol.	3094	264	338	150	40	44	14
	Preselected	39340	63982	761926	269666	87932	63499	17562
70	After cuts	8608	424	320	146	58	36	64
	+ jet isol.	6266	262	206	90	40	24	52
	Preselected	56764	111512	970710	346349	117816	91416	38872
100	After cuts	11452	280	124	92	24	24	136
	+ jet isol.	9672	204	92	64	24	20	120

Table 4: Efficiency, S/B ratio and significance values in the selected events without jet isolation cut.

$\hat{p}_\perp^{min}$ (GeV/c)	S	B	$Eff_S(\%)$	$Eff_B(\%)$	S/B	$S/\sqrt{B}$
40	6238	2122	34.55±0.51	0.831±0.018	2.9	135.4
70	8608	984	21.88 ± 0.26	0.079 ± 0.003	8.8	274.4
100	11452	544	20.17 ± 0.21	0.033 ± 0.001	21.1	491.0

Table 5: Efficiency, S/B ratio and significance values in the selected events with jet isolation cut.

$\hat{p}_\perp^{min}$ (GeV/c)	S	B	$Eff_S(\%)$	$Eff_B(\%)$	S/B	$S/\sqrt{B}$
40	3094	836	17.14±0.33	0.327±0.011	3.7	107.0
70	6266	622	15.93 ± 0.22	0.050 ± 0.002	10.1	251.2
100	9672	404	17.04 ± 0.19	0.025 ± 0.001	23.9	481.2

Table 3 includes the numbers of signal and background events left in three generated event samples after application of cuts 1–16 and 1–17. They are given for all three intervals of $P_t^{\tilde{\gamma}}$. The summary of Table 2 is presented in the middle section ($\hat{p}_\perp^{min} = 70$ GeV/c) of

---

[5]One must keep in mind that the starting value of S/B ratio has a model dependent nature.

[6]See [1] and [2] for a detailed definitions of P_t^{out} and jet isolation parameter ϵ^{jet}.

Table 3 where the line "Preselected" corresponds to the cut 1 of Table 1 and, respectively, to the line number 1 of Table 2 presented above. The line "After cuts" corresponds to the line 16 of Table 2 and line "+jet isolation" corresponds to the line 17 of Table 2.

Table 3 shows in more detail the origin of γ^{dir}-candidates. The numbers in the column "$\gamma - direct$" correspond to the numbers of signal events caused by QCD subprocesses (1) and (2) left in each of $P_t^{\tilde{\gamma}}$ intervals after application of the cuts defined in lines 1, 16 and 17 of Table 1 (see also column "S" of Table 2). Analogously, the numbers in the column "$\gamma - brem$" of Table 3 correspond to the numbers of events with the photons radiated from quarks participating in hard $2 \rightarrow 2$ parton interactions. Columns 5 – 8 of Table 3 illustrate the numbers of the "$\gamma - mes$" events with photons originating from π^0, η, ω and K_S^0 meson decays. In a case of $\hat{p}_\perp^{min} = 40 \ GeV/c$ the total numbers of background events, i.e. a sum over the numbers presented in columns 4 – 8 of Table 3, are shown in lines 1, 16 and 17 of column "B" of Table 2.

The other lines of Table 3 for $\hat{p}_\perp^{min} = 40$ and $100 \ GeV/c$ have the meaning analogous to that one described above for $\hat{p}_\perp^{min} = 70 \ GeV/c$.

The last column of Table 3 shows the number of preselected events with γ^{dir}-candidates faked by $e^\pm$. One can see that at $\hat{p}_\perp^{min} = 40 \ GeV/c$ their contribution at the level of the last cut "+jet isol." of Table 3 (or cut 17 of Table 1) to the value of the considered total background is about 2% and grows up to 30% at $\hat{p}_\perp^{min} = 100 \ GeV/c$. Furhter suppression of the events with $\tilde{\gamma} = e^\pm$ depends on the value of track finding efficiency.

Here we take the efficiency of each cut of Table 1 to be equal to 100% as we study the results of simulation at the particle level. For estimation of the size of possible detector effects one may take into account the value of a track finding efficiency in the central region ($|\eta| < 0.9$) of D0 detector ([8], [9]) found in Run I to be about 83%.

The numbers in Tables 4 (without jet isolation cut) and 5 (with jet isolation cut) accumulate in a compact form the final information of Tables 1 – 3. So, for example, the values in columns S and B for $\hat{p}_\perp^{min} = 70 \ GeV/c$ include the total numbers of the selected signal and background events taken correspondingly at the level of 16-th (for Table 4) and 17-th (for Table 5) cuts from Table 2.

It is seen from Table 4 that the ratio S/B grows from 2.9 to 21.1 while $P_t^{\tilde{\gamma}}$ increases from $P_t^{\tilde{\gamma}} \geq 40 \ GeV/c$ to $P_t^{\tilde{\gamma}} \geq 100 \ GeV/c$ interval.

The jet isolation requirement (cut 17 from Table 1) noticeably improves the situation at low $P_t^{\tilde{\gamma}}$ (see Table 5). After application of this criterion the value of S/B increases from 2.9 to 3.7 at $P_t^{\tilde{\gamma}} \geq 40 \ GeV/c$ while at $P_t^{\tilde{\gamma}} \geq 100 \ GeV/c$ the value of S/B changes only from 21.1 to 23.9 due to a tendency of the selected event sample to contain more events with an isolated jet as $P_t^{\tilde{\gamma}}$ increases (see [1] and [2]).

Let us underline here that, *in contrast to other types of background, the "$\gamma - brem$" background has an irreducible nature.* Thus, the number of "$\gamma - brem$" events should be carefully estimated for each $P_t^{\tilde{\gamma}}$ interval using the particle level of simulation in the framework of event generators like PYTHIA. The contribution of "$\gamma - brem$" background must be taken into account in analysis of the experimental data on prompt photon production especially for high P_t intervals where, as it is seen from Table 3, it becomes a dominant one as compared with the contribution from "$\gamma - mes$" and "$e^\pm$" events [7].

---

[7]For a careful theoretical study of '$\gamma - brem$" background to direct photon production see [10, 11] and the corresponding references in them.

2 Event rates estimation at the Tevatron.

One of the promising channels for measurement of the proton gluon density, as was shown in [12], is a high P_t direct photon production $p\bar{p}(p) \rightarrow \gamma^{dir} + X$. The region of high P_t, reached by UA1 [13], UA2 [14], CDF [15] and D0 [8] extends up to $P_t \approx 60\ GeV/c$ and recently up to $P_t = 105\ GeV/c$ [9]. These data together with the later ones (see references in [16]–[24]) and recent E706 [25] and UA6 [26] results give an opportunity for tuning the form of gluon distribution (see [17], [20], [27]). The rates and estimated cross sections of inclusive direct photon production at the LHC are given in [12] (see also [28]).

Here for the same aim we consider the process $p\bar{p} \rightarrow \gamma^{dir} + 1\,jet + X$ defined in the leading order by two QCD subprocesses (1) and (2) (for experimental results see [29], [30] and references in [31]). The analogous study for LHC energy was done in [2],[3] and [31].

The "$\gamma^{dir} + 1\,jet$" final state is more preferable than inclusive photon production $\gamma^{dir} + X$ from the viewpoint of extraction of information on gluon distribution. Indeed, in the case of inclusive direct photon production the cross section is given as an integral over partons distribution functions $f_a(x_a, Q^2)$ (a = quark or gluon), while in the case of $p\bar{p} \rightarrow \gamma^{dir} + 1\,jet + X$ for $P_t^{jet} \geq 30\,GeV/c$ (i.e. in the region where "k_t" smearing effects are not important, see [21]) the cross section is expressed directly in terms of these distributions (see, for example, [19]):

$$\frac{d\sigma}{d\eta_1 d\eta_2 dP_t^2} = \sum_{a,b} x_a\, f_a(x_a, Q^2)\, x_b\, f_b(x_b, Q^2) \frac{d\sigma}{d\hat{t}}(a\,b \rightarrow 3\,4), \qquad (3)$$

where

$$x_{a,b} = P_t/\sqrt{s} \cdot (exp(\pm\eta_1) + exp(\pm\eta_2)). \qquad (4)$$

We used the following designations above: $\eta_1 = \eta^\gamma$, $\eta_2 = \eta^{jet}$; $P_t = P_t^\gamma$; a,b = $q, \bar{q}, g$; 3,4 = $q, \bar{q}, g, \gamma$. Formula (3) and the knowledge of the results of independent measurements of q, $\bar{q}$ distributions allow the gluon distribution $f_g(x, Q^2)$ to be determined after account of selection efficiencies of γ^{dir}-candidates and the contribution of background, left after the used selection cuts (1–13 of Table 1), as it was discussed in Section 1 keeping in mind this application.

In the previous works (e.g. see [1]–[3]) a lot of details connected with the structure and topology of these events and the objects appearing in them were discussed. Having all this information we are in position to discuss an application of the "$\gamma + jet$" event samples selected with the proposed cuts and to estimate the rates of gluon-based subprocess (1).

Table 6 shows the percentage of "Compton-like" subprocess (1) (amounting to 100% together with (2)) in the samples of generated with PYTHIA events and then selected with cuts 1 – 13 of Table 1 for different P_t^γ and η^{jet} intervals: Central (CC, $|\eta| < 0.7$), Intercryostat (IC, $0.7 < |\eta| < 1.8$) and End (EC, $1.8 < |\eta| < 2.5$) calorimeter.

Table 6: The percentage of "Compton-like" process $q\,g \rightarrow \gamma + q$.

Calorimeter	P_t^γ interval (GeV/c)			
part	40–50	50–70	70–90	90–140
CC	84	80	74	68
IC	85	82	76	70
EC	89	85	82	73

In Table 7 we present the $Q^2 (\equiv (P_t^\gamma)^2)$ and x (defined according to (4)) distribution of the number of events (for integrated luminosity $L_{int} = 3\ fb^{-1}$) that are caused by

6

subprocess (1) and passed cuts 1 – 13 of Table 1 with $P_t^{isol} < 4\ GeV/c$ and $\epsilon^\gamma < 7\%$ (applied in the line 5) [8].

The analogous information for events caused by (1) with the charmed quarks $g\,c \to \gamma^{dir} + c$ is presented in Table 8. The simulation of the process $g\,b \to \gamma^{dir} + b$ shows that the rates for b-quark are $8 - 10$ times lower than those for c-quark.

Table 7: Number of $g\,q \to \gamma^{dir} + q$ events at different Q^2 and x intervals for $L_{int} = 3\ fb^{-1}$.

Q^2	x values of a parton						All x
$(GeV/c)^2$	$.001 - .005$	$.005 - .01$	$.01 - .05$	$.05 - .1$	$.1 - .5$	$.5 - 1.$	$.001 - 1.$
1600-2500	8582	56288	245157	115870	203018	3647	632563
2500-4900	371	13514	119305	64412	119889	3196	320688
4900-8100	0	204	17865	13514	26364	1059	59007
8100-19600	0	0	3838	5623	11539	548	21549
							1 033 807

Table 8: Number of $g\,c \to \gamma^{dir} + c$ events at different Q^2 and x intervals for $L_{int} = 3\ fb^{-1}$.

Q^2	x values of a parton						All x
$(GeV/c)^2$	$.001 - .005$	$.005 - .01$	$.01 - .05$	$.05 - .1$	$.1 - .5$	$.5 - 1.$	$.001 - 1.$
1600-2500	264	2318	21236	11758	14172	58	49805
2500-4900	13	332	9522	6193	7785	40	23885
4900-8100	0	4	914	1055	1648	16	3637
8100-19600	0	0	142	329	612	8	1092
							78 419

Fig. 1 shows in the widely used (x, Q^2) kinematic plot (see [32]) what area can be covered by studying the process $q\,g \to \gamma + q$. The number of expected events in this area is given in Table 7. From this figure and Table 7 it becomes clear that at integrated lumin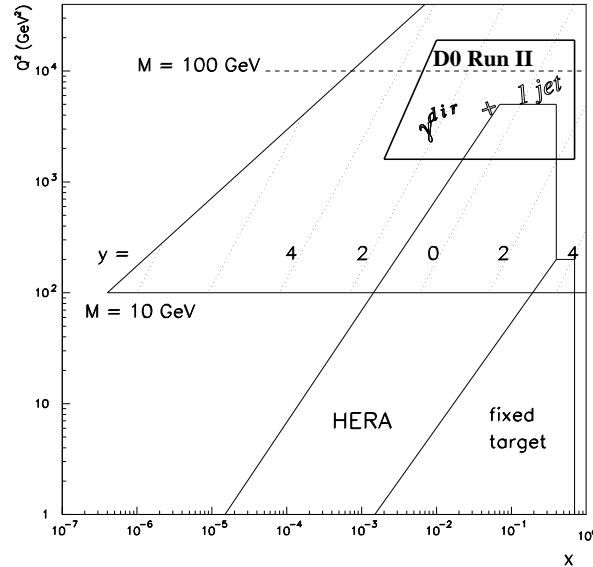osity $L_{int} = 3\ fb^{-1}$ it would be possible to study the gluon distribution with good statistics of "$\gamma + jet$" events in the region of small x at Q^2 about one order of magnitude higher than now reached at HERA [33], [34]. It is worth emphasizing that extension of the experimentally reachable region at the Tevatron to the region of lower Q^2 overlapping with the area covered by HERA would also be of great interest (for instance, it would allow to test analytical solutions of DGLAP equations that describe Q^2-evolution of structure functions at small values of x [35].

Figure 1: The (x, Q^2) kinematic region for $p\bar{p} \to \gamma^{dir} + jet$ process.

---

[8]An application of cuts 14–17, as it is seen from Table 2, leads only to 20% improvement of S/B ratio.

Acknowledgments.

References

[1] D.V. Bandurin, N.B. Skachkov. "$\gamma + jet$" process application for setting the absolute scale of jet energy and determining the gluon distribution at the Tevatron Run II." D0 Note 3948, 2002, hep-ex/0203003.

[2] D.V. Bandurin, V.F. Konoplyanikov, N.B. Skachkov. "Jet energy scale setting with "$\gamma + jet$" events at LHC energies." JINR Preprint E2-2000-251 – E2-2000-255, JINR, Dubna, hep-ex/0011012, hep-ex/0011013, hep-ex/0011014, hep-ex/0011017, hep-ex/0011084.

[3] D.V. Bandurin, V.F. Konoplyanikov, N.B. Skachkov, "$\gamma + jet$" events rate estimation for gluon distribution determination at LHC", Part.Nucl.Lett.103:34-43,2000, hep-ex/0011015.

[4] Talk at D0 QCD group meeting, see http://www-d0.fnal.gov/Run2Physics/qcd/, link to "Meeting June 21, 2001".

[5] Talk at D0 QCD group meeting, see http://www-d0.fnal.gov/Run2Physics/qcd/, link to "Meeting February 25, 2002".

[6] T. Sjostrand, Comp.Phys.Comm. **82** (1994)74.

[7] The D0 Detector,Nucl.Instrum.Meth.A338:185-253,1994.

[8] D0 Collaboration, F. Abachi *et al.*, Phys.Rev.Lett, **77** (1996)5011;

[9] D0 Collaboration, B. Abbott *et al.* , Phys.Rev.Lett. **84** 2786-2791,2000.

[10] E.L. Berger and J. Qiu, Phys.Rev. **D44** (1991)2002.

[11] P. Aurenche *et al.* , hep-ex/9811382, 1998.

[12] P. Aurenche *et al.* Proc. of "ECFA LHC Workshop", Aachen, Germany, 4-9 October 1990, edited by G. Jarlskog and D. Rein (CERN-Report No 90-10; Geneva, Switzerland 1990), Vol. **II**

[13] UA1 Collaboration, C. Albajar *et al.*, Phys.Lett, **209B** (1998)385.

[14] UA2 Collaboration, R. Ansari *et al.*, Phys.Lett. **176B** (1986)239.

[15] CDF Collaboration. F. Abe *et al.*, Phys.Rev.Lett. **68** (1992)2734; F. Abe *et al.*,Phys.Rev. **D48** (1993)2998; F. Abe *et al.*,Phys.Rev.Lett., **73** (1994)2662.

[16] T. Ferbel and W.R. Molzon, Rev.Mod.Phys. **56** (1984)181.

[17] P. Aurenche, *et al.* Phys.Lett. **169B** (1986)441.

[18] E.N. Argyres, A.P. Contogouris, N. Mebarki and S.D.P. Vlassopulos, Phys.Rev, **D35** (1987)1534–1589.

[19] J.F. Owens, Rev.Mod.Phys. **59** (1987)465.

[20] W. Vogelsang and A. Vogt, Nucl.Phys. **B453** (1995)334.

[21] J. Huston ATLAS Note ATL-Phys-99-008, CERN,1999.

[22] J. Huston *et al.* "Study of the uncertainty of the gluon distribution", hep-ph/9801444.

[23] W. Vogelsang and M. Whally, J.Phys. **G23** (1997)A1.

[24] S. Frixione and W. Vogelsang, CERN-TH/99-247 hep-ph/9908387.

[25] E706 Collaboration, L. Apanasevich *et al.*, Phys.Rev.Lett., **81** (1997)2642.

[26] UA6 Collaboration, G. Ballocchi *et al.*, Phys.Lett.,**B436** (1998)222.

[27] A.D. Martin *et al.*, Eur.Phys.J. **C4** (1998)463.

[28] P. Aurenche, M. Fontannaz, S. Frixione Proc. of "CERN Workshop on Standard Model Physics (and more) at the LHC", QCD, Section 6.1 "General features of photon production", Yellow Report CERN-2000-004, 9 May 2000, CERN, Geneva.

[29] ISR–AFS Collaboration, T.Akesson *et al.*, Zeit.Phys. **C34** (1987)293;

[30] CDF Collaboration, F. Abe *et al.*,Phys.Rev. **D57** (1998)67.

[31] M. Dittmar, K.Mazumdar, N. Skachkov, Proc. of "CERN Workshop on Standard Model Physics (and more) at the LHC", QCD, Section 2.7 "Measuring parton luminosities and parton distribution functons at the LHC", Yellow Report CERN-2000-004, May 2000, CERN, Geneva.

[32] R. Ball, M. Dittmar, W.J. Stirling, Proc. of "CERN Workshop on Standard Model Physics (and more) at the LHC", QCD, Section 2 "Parton distribution functons", Yellow Report CERN-2000-004, May 2000, CERN, Geneva.

[33] H1 Collaboration, S. Aid *et al.*, Nucl.Phys. **B470** (1996)3; C. Adloff *et al.* Nucl.Phys. **B497** (1997)3.

[34] ZEUS Collaboration, M. Derrick *et al.*, Zeit.Phys. **C69** (1996)607; M. Derrick *et al.*, Zeit.Phys. **C72** (1996)399.

[35] A.V. Kotikov and G. Parente, Nucl.Phys.**B549** (1999)242-262.